Journal of Thermal Analysis and Calorimetry (2020) 140:2317–2324
https://doi.org/10.1007/s10973-019-09015-9

# A study on kinetics of ignition reaction of $B_4C/KNO_3$ and $B_4C/KClO_4$ pyrotechnic smoke compositions

**Jingran Xu[1] · Chenguang Zhu[1] · Xiao Xie[1] · Chenguang Yan[1] · Yikai Wang[1]**

Received: 15 May 2019 / Accepted: 1 November 2019 / Published online: 9 November 2019


**Abstract**
Presented herein is a study on the ignition reaction kinetics and mechanism of $B_4C/KNO_3$ and $B_4C/KClO_4$ pyrotechnic smoke compositions using the non-isothermal thermogravimetry and differential scanning calorimetry techniques. The pyrotechnics in oxygen balance of − 10%, − 20% and − 30% were prepared for the experiments. The results of measurements showed that the pyrotechnics in oxygen balance of − 20% had the highest enthalpy. The activation energy ($E_a$) of ignition reactions was calculated by using Ozawa–Flynn–Wall (OFW) and Kissinger–Akahira–Sunose (KAS) methods. The $E_a$ values of $B_4C/KNO_3$ and $B_4C/KClO_4$ were 139.5 and 214.6 kJ mol$^{-1}$ calculated by OFW method, and 129.3 and 210.7 kJ mol$^{-1}$ by KAS method. The differential and integral reaction mechanism functions of $B_4C/KNO_3$ and $B_4C/KClO_4$ were determined, respectively, by $z(\alpha)$ master plots method, $f_1(\alpha)=2(1-\alpha)[-\ln(1-\alpha)]^{1/2}$, $g_1(\alpha)=[-\ln(1-\alpha)]^{1/2}$, and $f_2(\alpha)=3(1-\alpha)[-\ln(1-\alpha)]^{2/3}$, $g_2(\alpha)=[-\ln(1-\alpha)]^{1/3}$. The pre-exponential factors, $\ln A=11.6$ and 22.3 min$^{-1}$, were obtained by the intercept of KAS method for ignition reaction of $B_4C/KNO_3$ and $B_4C/KClO_4$ pyrotechnics. Based on the results, the burning rates, thermal sensitivities and application methods of $B_4C/KNO_3$ and $B_4C/KClO_4$ were predicted.

**Keywords** Pyrotechnics · TG/DSC · Ignition reaction · Kinetics

## Introduction

Pyrotechnic smoke compositions are used for signaling, for obscuring targets and troop movements and for interfering with optical detection equipment. For many years, red phosphorus smoke compositions, white phosphorus smoke compositions and hexachloroethane smoke compositions were widely used in battlefield. However, $P_2O_5$ (the combustion product of P) is notoriously toxic and corrosive; white phosphorus itself is incendiary and toxic and can cause air pollution and water pollution; hexachloroethane and chlorinated organics have been responsible for several injuries and deaths [1]. Exploring an environment-friendly pyrotechnic fuel is the research focus in recent years. An advanced and versatile boron carbide-based visual obscurant composition was introduced by Shaw et al. [2, 3]. Boron carbide was considered as a new pyrotechnic fuel with good visible extinction properties, low toxicity and low damage to environment in smoke compositions. Thus, the ignition reaction kinetics of $B_4C/KNO_3$ and $B_4C/KClO_4$ pyrotechnic smoke compositions is the focus in this study.

Boron carbide ($B_4C$) has a high melting point of 2763 °C and a high boiling point of 3500 °C and high stability to most chemicals [4]. Potassium nitrate ($KNO_3$) is a white crystalline solid with a melting point of 334 °C and a boiling point of 400 °C [5]. It is a little hygroscopic, so it should be dried before mixing. Potassium perchlorate ($KClO_4$) is a white crystalline non-hygroscopic material with a melting point of 610 °C, but decomposes from 400 °C [6].

The oxygen balance (OB) of a pyrotechnic composition is an important factor that has influence on the ignition reaction. For pyrotechnic smoke compositions, more complete the ignition reaction is, more smoke can be produced. Pyrotechnic compositions are usually ignited in the air atmosphere. The stability and safety of pyrotechnics decrease with the increase in oxidant. Obtaining high enthalpy and completed reaction are two important principles for determining oxygen balance. Thus, the oxygen balance is generally − 10% to − 30% [7].

Thermal analysis methods are characterization techniques that can indicate the variation in macro-average properties of

✉ Chenguang Zhu
zcg_lnkz@163.com

[1] School of Chemical Engineering, Nanjing University of Science and Technology, Nanjing 210094, China

samples with temperature [8]. Thermal analysis methods of thermogravimetry (TG), differential thermal analysis (DTA) and differential scanning calorimetry (DSC) can be applied to study the mechanism and kinetics of thermal ignition reaction of energetic materials such as pyrotechnic smoke compositions [9]. The thermal analysis results of ignition reaction of energetic materials such as pyrotechnic compositions can be used to predict the quality, burning rate, shelf life and thermal hazard potential of them [10].

The method of studying the kinetics of ignition reaction by thermal analysis is to determine the kinetic triplet (activation energy $E_a$, pre-exponential factor $A$ and the reaction mechanism function $f(\alpha)$) [11, 12]. For ignition reaction of $B_4C/KNO_3$ and $B_4C/KClO_4$ pyrotechnics, model-free methods can be used to calculate the $E_a$ values without knowing the reaction models and pre-exponential factors. Then, pre-exponential factor $A$ and the reaction mechanism function $f(\alpha)$ can be determined by $z(\alpha)$ master plots method.

## Experiments

### Materials preparation

The $B_4C$ powder with purity > 99% was purchased from Meryer Chemical Technology Co., Ltd., and the $KNO_3$ and $KClO_4$ powder with purity > 99.7% were purchased from Sinopharm Chemical Reagent Co., Ltd. The particle size of $B_4C$, $KNO_3$ and $KClO_4$ were 1250 mesh (12 μm), 200 mesh (74 μm) and 280 mesh (53 μm). $KNO_3$ was ground into fine powder in a mortar and sifted and then was dried at 80 °C for 3 h. Fuel ($B_4C$) and oxidant ($KNO_3$ and $KClO_4$) were mixed in a mortar for 10 min in the oxygen balance of − 10%, − 20% and − 30%. (The mass ratios of $B_4C$ to $KNO_3$ are 23:77, 28:72 and 33:67; the mass ratios of $B_4C$ to $KClO_4$ are 26:74, 30:70 and 35:65.)

### Instruments

The TG/DSC measurements were carried out with NETZSCH STA 449C F3 simultaneous thermal analyzer made in Germany.

### Experiments condition

Samples of $B_4C/KNO_3$ and $B_4C/KClO_4$ with a mass of about 2 mg were employed for these measurements. Platinum pans with 50 mL volume were used as sample containers. The samples were measured in the high-purity argon atmosphere with flow rate of 50 mL $min^{-1}$. The samples were heated from ambient temperature (30 °C) to 700 °C at different heating rates of 5, 10, 15 and 20 K $min^{-1}$. Five repeated TG/DSC experiments were carried out to avoid errors.

## Results and discussion

### TG/DSC curves of pyrotechnic compositions at different oxygen balance

The TG/DSC curves in Figs. 1 and 2 illustrate the thermal behavior of $B_4C/KNO_3$ and $B_4C/KClO_4$ in different oxygen balance at heating rate of 15 K $min^{-1}$. The data obtained from five repeated experiments are highly consistent. The curves show that solid-phase boron carbide with high melting point and high boiling point reacted with $KNO_3$ and $KClO_4$ in about 495 and 547 °C. The curves indicate that ignition reactions of two compositions take place via one stage with a mass loss amounts to about 13% and 30.5%. The mass loss of $B_4C/KNO_3$ is compatible with that theoretically anticipated one according to the suggested decomposition equation [13]:

$$2KNO_3 \rightarrow 2KNO_2 + O_2$$
$$B_4C + 4KNO_2 \rightarrow 4KBO_2 + 2N_2 \uparrow + C$$
$$B_4C + 3O_2 \rightarrow 2B_2O_3 + C$$
$$5B_4C + 12KNO_3 \rightarrow 12KBO_2 + 6N_2 \uparrow + 4B_2O_3 + 5C$$

The mass loss of $B_4C/KClO_4$ is inconsistent with the predicted chemical reaction equation [14, 15]:

$$KClO_4 \rightarrow KCl + 2O_2$$
$$B_4C + 3O_2 \rightarrow 2B_2O_3 + C$$
$$2B_4C + 3KClO_4 \rightarrow 3KCl + 4B_2O_3 + 2C$$

The difference between the theoretical and predicted mass loss was analyzed. It is inferred that the cause leading to this result is the loss of oxygen gases, because the bonding of $B_4C/KNO_3$ and $B_4C/KClO_4$ particles is not close enough.

The initial temperature ($T_o$), peak temperature ($T_p$), final temperature ($T_f$) and the enthalpy values ($\Delta T$) are shown in Table 1. Under the same heating rate, characteristic temperatures are similar between compositions in different oxygen balance. The DSC data show that the highest enthalpy for ignition reaction of $B_4C/KNO_3$ and $B_4C/KClO_4$ is both obtained in oxygen balance of − 20%. Besides, the TG curves indicated that the mass reduction of $B_4C/KNO_3$ and $B_4C/KClO_4$ in OB of − 20% was about 12% and 29% that was more than the mass reduction in others. Thus, the ignition reactions of $B_4C/KNO_3$ and $B_4C/KClO_4$ in OB of − 20% were most completed.

### Calculation for activation energy of ignition reaction

The obtained data indicate that $B_4C/KNO_3$ and $B_4C/KClO_4$ in oxygen balance of − 20% have the highest enthalpy values

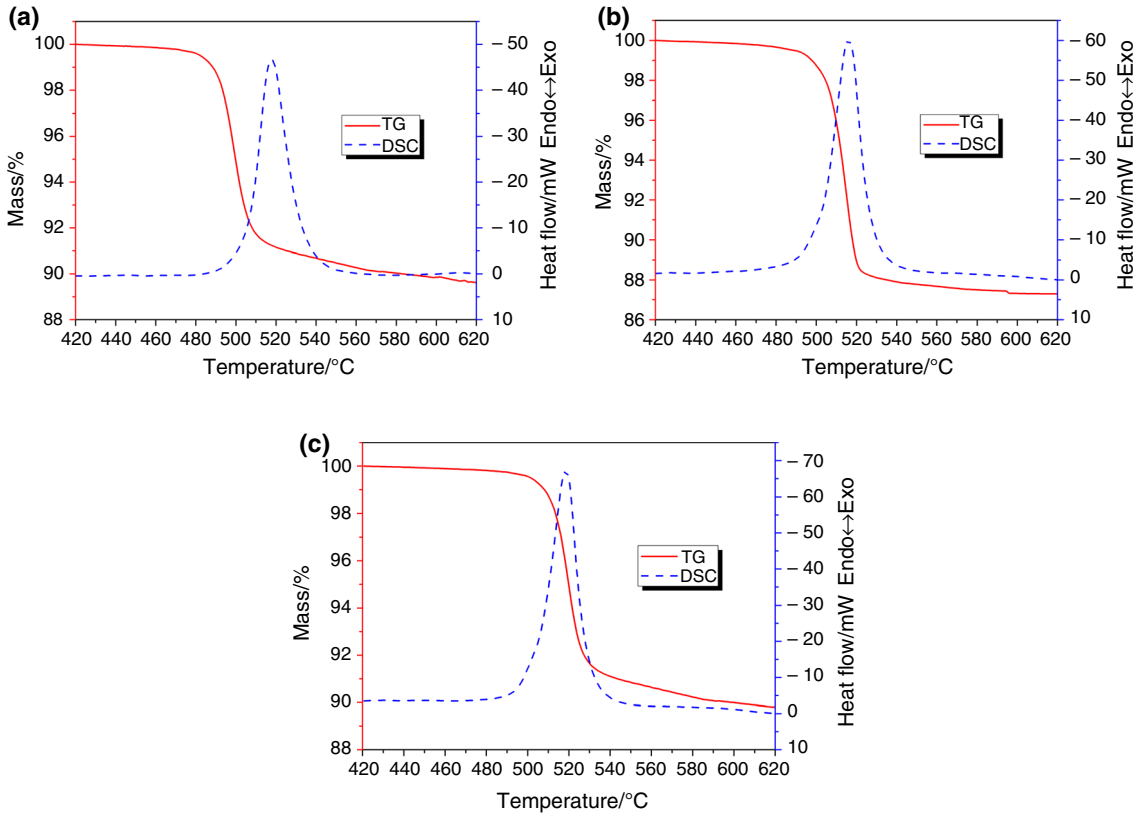


**Fig. 1** TG/DSC curves of $B_4C/KNO_3$ pyrotechnic compositions in OB of − 10%, − 20% and − 30%

($\Delta H$). Therefore, this oxygen balance was used to study the ignition reaction kinetics. Figures 3 and 4 show the DSC curves of $B_4C/KNO_3$ and $B_4C/KClO_4$ under heating rates of 5, 10, 15 and 20 K $min^{-1}$. The initial temperature ($T_o$), peak temperature ($T_p$) and final temperature ($T_f$) with different heating rates are recorded in Table 2. With the increase in heating rate, $T_o$, $T_p$ and $T_f$ are all delayed.

Under non-isothermal conditions, the reaction kinetics equation in heterogeneous systems is represented as Eq. 1:

$$\frac{d\alpha}{dT} = \left(\frac{A}{\beta}\right) \exp\left(-\frac{E_a}{RT}\right) f(\alpha) \tag{1}$$

where $\alpha$ is the conversion factor, $\beta$ *is* the heating rate, $R$ is the molar gas constant, $E_a$ is the activation energy, $A$ is the pre-exponential factor and $f(\alpha)$ is the reaction mechanism function. The calculation of the kinetic triplet is essential to analyze the reaction kinetics.

In this study, the activation energy ($E_a$) of ignition reactions of $B_4C/KNO_3$ and $B_4C/KClO_4$ pyrotechnics was calculated by using Ozawa–Flynn–Wall (OFW) and Kissinger–Akahira–Sunose (KAS) methods. The FWO and KAS methods can directly calculate the activation energy ($E_a$) without the reaction mechanism function ($f(\alpha)$), thereby avoiding the errors caused by different assumptions of reaction mechanism functions. The OFW method is represented as Eq. 2 developed by Ozawa [16] and Flynn and Wall [17].

$$\lg \beta = \lg\left(\frac{AE_a}{RG(\alpha)}\right) - 2.315 - 0.4567\frac{E_a}{RT_p} \tag{2}$$

where $T_p$ is the peak temperature. Figure 5 shows the plots of log$\beta$ versus $1/T_p$ of $B_4C/KNO_3$ and $B_4C/KClO_4$, respectively. $E_a$ values can be obtained by calculating the slopes of the plots. The $E_a$ values of $B_4C/KNO_3$ and $B_4C/KClO_4$ are 139.5 kJ $mol^{-1}$ and 214.6 kJ $mol^{-1}$.

Compared to the OFW method, the KAS method offers a significant improvement in the accuracy of the $E_a$ values [18, 19].

$$\ln\left(\frac{\beta_i}{T_{\alpha,i}^2}\right) = \ln\frac{AR}{E_a g(\alpha)} - \frac{E_{a,\alpha}}{RT_{\alpha,i}} \tag{3}$$

The curves of temperature versus conversion ($\alpha - T$) at heating rates ($\beta_i$) of 5, 10, 15 and 20 K $min^{-1}$ for thermal ignition of $B_4C/KNO_3$ and $B_4C/KClO_4$ are shown in Fig. 6 that illustrate the temperatures at different conversion factors ($T_{\alpha,i}$). At different conversions ($\alpha = 0.1$–$0.9$), nine

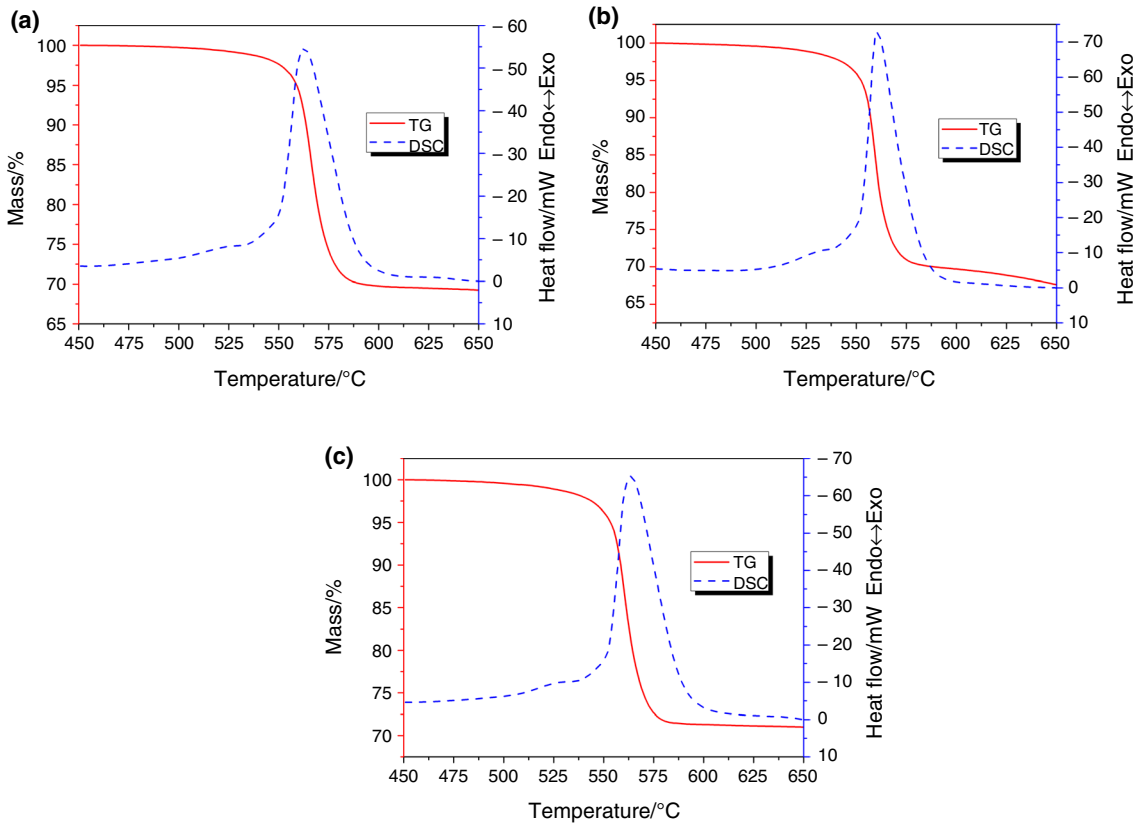


**Fig. 2** TG/DSC curves of $B_4C/KClO_4$ pyrotechnic compositions in OB of − 10%, − 20% and − 30%

**Table 1** Initial temperature ($T_o$), peak temperature ($T_p$), final temperature ($T_f$) and the enthalpy values ($\Delta H$) of pyrotechnic compositions

| Pyrotechnic compositions | $T_o$/°C | $T_p$/°C | $T_f$/°C | $\Delta H$/J g$^{-1}$ |
|---|---|---|---|---|
| $B_4C/KNO_3$ | 495.8 | 517.5 | 536.1 | 1739 |
| | 493.2 | 515.4 | 532.5 | 2131 |
| | 495.0 | 518.3 | 535.2 | 1965 |
| $B_4C/KClO_4$ | 542.9 | 562.4 | 590.1 | 1825 |
| | 543.2 | 560.4 | 590.0 | 1977 |
| | 547.9 | 563.9 | 589.8 | 1919 |

straight lines can be drawn by fitting the $\ln\left(\frac{\beta_i}{T^2_{\alpha,i}}\right) - \frac{1}{T_{\alpha,i}}$ in Fig. 7. As shown in Table 3, $E_a$ values at different conversions were calculated according to the slopes of lines.

It is obvious that the activation energy for ignition reaction of both $B_4C/KNO_3$ and $B_4C/KClO_4$ pyrotechnic compositions decreases with the conversion factors increase. This trend is closely related to the reaction mechanism and takes place when the overall reaction consists of several competitive or parallel reactions [10].

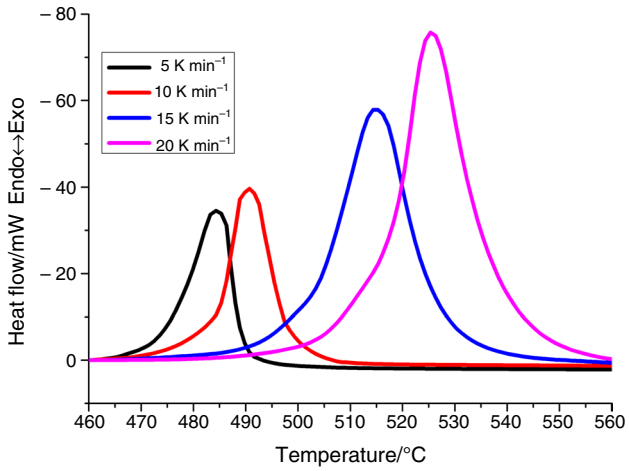


**Fig. 3** DSC curves of $B_4C/KNO_3$ under different heating rates of 5, 10, 15 and 20 K min$^{-1}$

The results indicate that the reaction rate increases with the progress of the ignition reaction. In terms of pyrotechnic smoke compositions for visible extinction, different ignition reaction rates are required in different situations. Furthermore, in the application of the pyrotechnic smoke

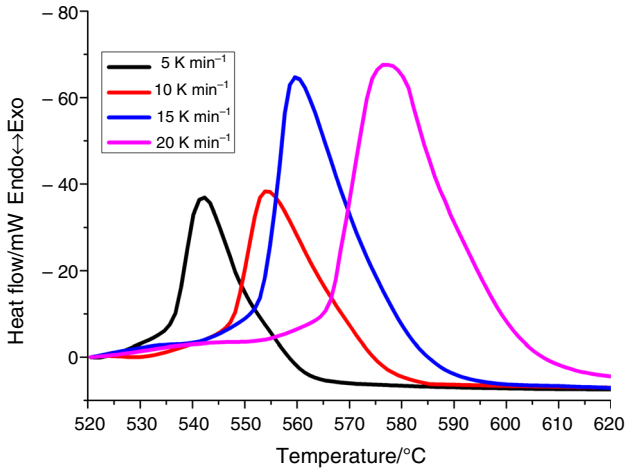


**Fig. 4** DSC curves of $B_4C/KClO_4$ under different heating rates of 5, 10, 15 and 20 K $min^{-1}$

**Table 2** Initial temperature ($T_o$), peak temperature ($T_p$) and final temperature ($T_f$) with different heating rates

| Pyrotechnic compositions | $\beta$/K $min^{-1}$ | $T_o$/°C | $T_p$/°C | $T_f$/°C |
|---|---|---|---|---|
| $B_4C/KNO_3$ | 5 | 472.5 | 484.3 | 489.8 |
| | 10 | 483.2 | 490.7 | 497.4 |
| | 15 | 500.4 | 514.3 | 529.3 |
| | 20 | 509.3 | 525.3 | 544.3 |
| $B_4C/KClO_4$ | 5 | 534.7 | 542.4 | 554.8 |
| | 10 | 545.3 | 553.8 | 574.3 |
| | 15 | 551.0 | 559.6 | 584.2 |
| | 20 | 564.4 | 577.3 | 602.3 |

compositions for infrared extinction, a high ignition reaction rate is always expected to disperse infrared extinction additives.

## Determination of kinetic triplet

The OFW and KAS methods are model-free methods that can evaluate the activation energy without accomplishing the reaction model. Pre-exponential factor $A$ and the reaction mechanism function $f(\alpha)$ can be determined by $z(\alpha)$ master plots method. The $z(\alpha)$ master plots (Eq. 6) are derived by combining the differential (Eq. 4) and integral forms (Eq. 5) of the reaction models [20]. The temperature integral in can be replaced with various approximations $\pi(x)$ as Eq. 5, where $x = \frac{E_{a,\alpha}}{RT_\alpha}$ [9, 21]:

$$\frac{d\alpha}{dT} = \frac{A}{\beta}\exp\left(-\frac{E}{RT}\right)f(\alpha) \tag{4}$$

$$g(\alpha) = \frac{A}{\beta}\int_0^T \exp\left(-\frac{E}{RT}\right)dT = \frac{AE}{\beta R}\exp(-x)\left[\frac{\pi(x)}{x}\right] \tag{5}$$

$$z(\alpha) = f(\alpha)g(\alpha) = \left(\frac{d\alpha}{dt}\right)_\alpha T_\alpha^2\left[\frac{\pi(x)}{\beta T_\alpha}\right] \tag{6}$$

The effect of the term in bracket of Eq. 6 is insignificant to the shape of the $z(\alpha)$ function plot [9]. Therefore, the $z(\alpha)$ values at different conversions $\alpha$ can be calculated by $\left(\frac{d\alpha}{dT}\right)_\alpha$ and $T_\alpha$ that result from the experiments. $z(\alpha)$ values are only dependent on $\alpha$ rather than the heating rate $\beta$, and thus, data of $\left(\frac{d\alpha}{dT}\right)_\alpha$ and $T_\alpha^2$ at four heating rates can obtain four experimental $z(\alpha)$ curves. As shown in Fig. 8, the plots of experimental $z(\alpha)$ values of $B_4C/KNO_3$ and $B_4C/KClO_4$ can be accomplished to compare against the theoretical $z(\alpha)$ master plots. The theoretical $z(\alpha)$ master plots in Fig. 9 show the $z(\alpha)$ master plots of Avrami–Erofeev reaction models for solid-state kinetics from Table 4 [22]. The best matches were obtained by calculating the minimum variances ($v^2$) between the experimental $z(\alpha)$ plots and the theoretical $z(\alpha)$ master plots. The differential and integral reaction mechanism functions of $B_4C/KNO_3$ and $B_4C/$

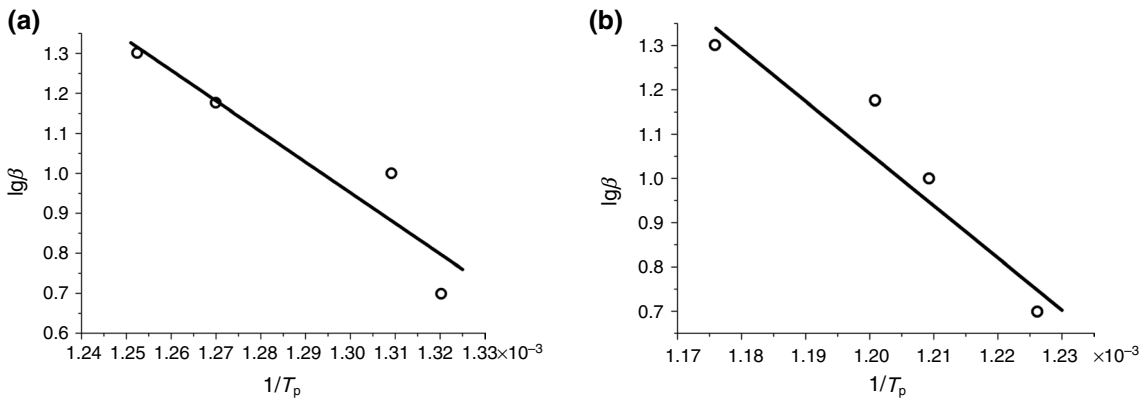


**Fig. 5** Fitting plots for log$\beta$ versus $1/T_p$ of $B_4C/KNO_3$ and $B_4C/KClO_4$ at four heating rates

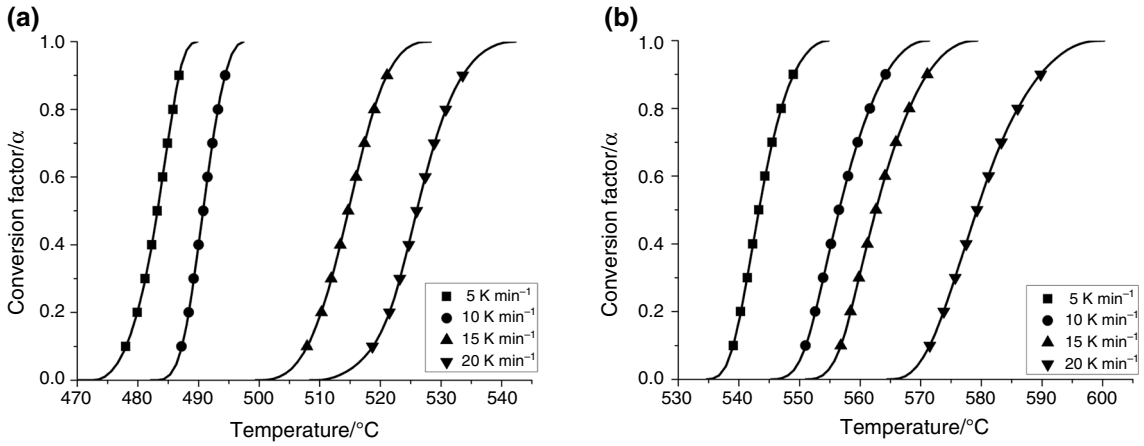


**Fig. 6** $\alpha$–$T$ curves of $B_4C/KNO_3$ and $B_4C/KClO_4$ at heating rates ($\beta_i$) of 5, 10, 15 and 20 K $min^{-1}$

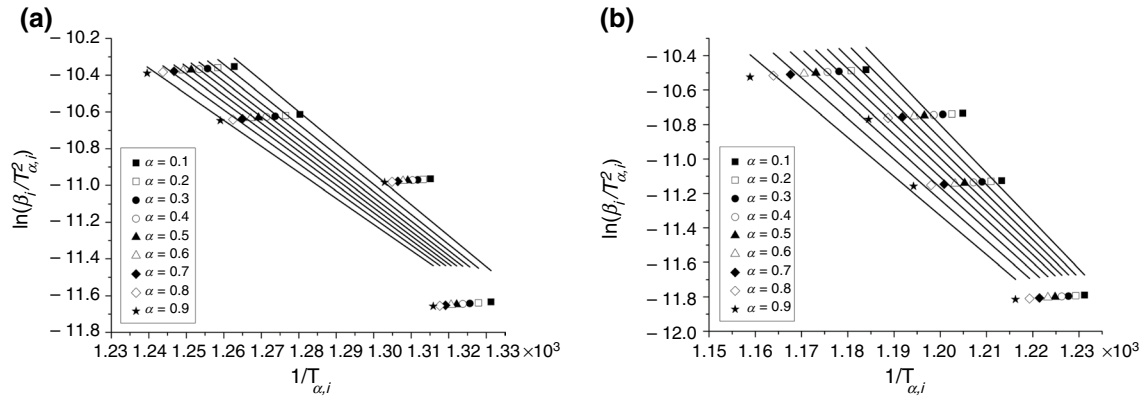


**Fig. 7** KAS method plots of $B_4C/KNO_3$ and $B_4C/KClO_4$ at various conversion factors ($\alpha$ = 0.1–0.9) and different heating rates ($\beta_i$) of 5, 10, 15 and 20 K $min^{-1}$

**Table 3** $E_a$ values of ignition reaction of $B_4C/KNO_3$ and $B_4C/KClO_4$ calculated by KAS method with $\alpha$ = 0.1–0.9

| $\alpha$ values | $E_a$ ($B_4C/KNO_3$)/kJ $mol^{-1}$ | $E_a$ ($B_4C/KClO_4$)/kJ $mol^{-1}$ |
|---|---|---|
| 0.1 | 140.5 | 232.2 |
| 0.2 | 135.8 | 225.3 |
| 0.3 | 133.3 | 219.9 |
| 0.4 | 131.4 | 215.1 |
| 0.5 | 129.6 | 210.6 |
| 0.6 | 127.7 | 206.4 |
| 0.7 | 125.7 | 202.0 |
| 0.8 | 122.4 | 196.1 |
| 0.9 | 117.9 | 188.7 |
| Average | 129.3 | 210.7 |

$KClO_4$ were determined, respectively, $f_1(\alpha) = 2(1-\alpha)[-\ln(1-\alpha)]^{1/2}$, $g_1(\alpha) = [-\ln(1-\alpha)]^{1/2}$, and $f_2(\alpha) = 3(1-\alpha)[-\ln(1-\alpha)]^{2/3}$, $g_2(\alpha) = [-\ln(1-\alpha)]^{1/3}$.

According to the reaction mechanism functions obtained, the pre-exponential factors, ln$A$ values, could be calculated using the KAS method. The slopes and intercepts of the fitting lines were obtained by KAS method before. The $E_a$ values were accomplished using the slopes, and ln$A$ values could be calculated by the intercepts that were equal to $\ln \frac{AR}{E_a g(\alpha)}$. The $E_a$ and $g(\alpha)$ were obtained before, and the ln$A$ values of ignition reaction of $B_4C/KNO_3$ and $B_4C/KClO_4$ pyrotechnics were 11.6 and 22.4 $min^{-1}$.

## The relation of results and smoke composition properties

The calculated kinetic triplet (activation energy $E_a$, pre-exponential factor ln$A$ and the reaction mechanism function

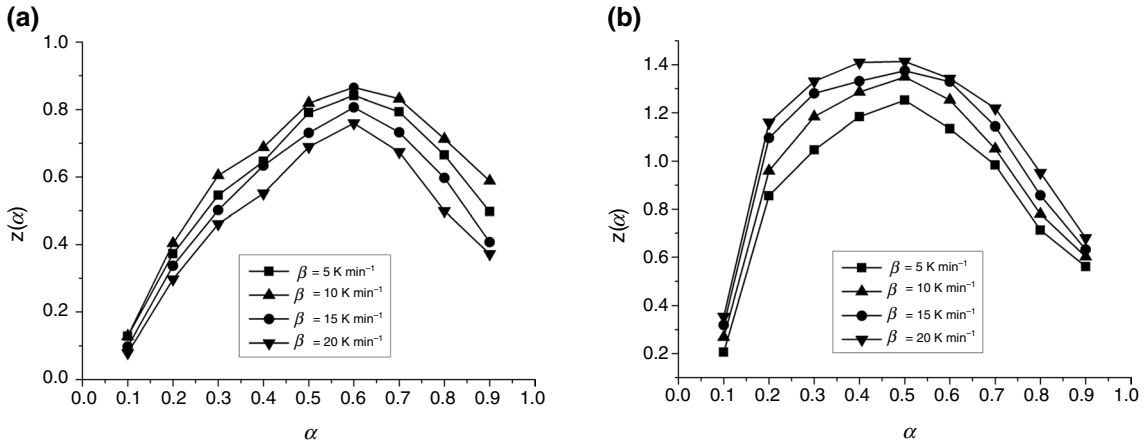


**Fig. 8** Plots of experimental $z(\alpha)$ values of $B_4C/KNO_3$ and $B_4C/KClO_4$ at heating rates of 5, 10, 15 and 20 K $min^{-1}$

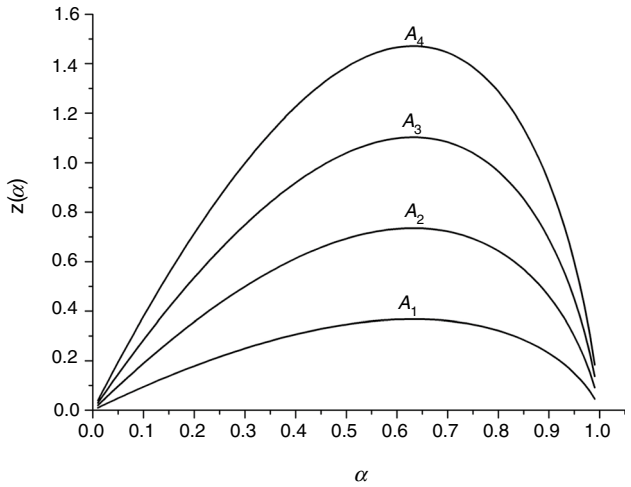


**Fig. 9** Theoretical $z(\alpha)$ master plots of Avrami–Erofeev reaction models for solid-state kinetics

**Table 4** Differential and integral reaction mechanism function of Avrami–Erofeev reaction models for solid-state kinetics

| Model | Differential forms | Integral forms |
|---|---|---|
| A1 | $f(\alpha)=1-\alpha$ | $g(\alpha)=-\ln(1-\alpha)$ |
| A2 | $f(\alpha)=2(1-\alpha)[-\ln(1-\alpha)]^{1/2}$ | $g(\alpha)=[-\ln(1-\alpha)]^{1/2}$ |
| A3 | $f(\alpha)=3(1-\alpha)[-\ln(1-\alpha)]^{2/3}$ | $g(\alpha)=[-\ln(1-\alpha)]^{1/3}$ |
| A4 | $f(\alpha)=4(1-\alpha)[-\ln(1-\alpha)]^{3/4}$ | $g(\alpha)=[-\ln(1-\alpha)]^{1/4}$ |

$f(\alpha)$) determines the burning rate of the composition. The thermal sensitivity can be reflected by the initial temperatures ($T_0$) shown by DSC curves of $B_4C/KNO_3$ and $B_4C/KClO_4$.

The results show that $B_4C/KNO_3$ has high thermal sensitivity and fast burning rate. This kind of smoke composition has both advantages and disadvantages. The disadvantages are that the compositions cannot maintain long-term smoke release, and the thermal sensitivity needs attention. The advantages are that binder and diluent can be added to reduce burning rate, increase the amount of smoke and improve safety. Furthermore, this smoke composition can be ignited well to achieve both visible and infrared obscuring when some nonflammable infrared extinction additives, such as $SiO_2$ powders and Cu powders, are added into composition.

The results show that $B_4C/KClO_4$ has low thermal sensitivity and low burning rate. The advantage is that it can produce a thick smoke screen and lasts a long time. It can be mixed with suitable binder and used directly to make visible obscuring products. The disadvantage is that any additives that can passivate smoke composition or lead to a decrease in burning rate will make the product difficult to ignite. Therefore, it is difficult for smoke compositions with $B_4C/KClO_4$ as fuel/oxidizer pair to achieve infrared obscuring.

## Conclusions

The non-isothermal TG/DSC experiments indicated that the ignition reaction of $B_4C/KNO_3$ and $B_4C/KClO_4$ pyrotechnics in OB of −20% showed the highest enthalpy. The kinetic parameters of ignition reaction of $B_4C/KNO_3$ and $B_4C/KClO_4$ pyrotechnics in OB of −20% were studied by TG/DSC technique at different heating rates of 5, 10, 15 and 20 K $min^{-1}$. The $E_a$ values of $B_4C/KNO_3$ and $B_4C/KClO_4$ calculated by OFW method were 139.5 and 214.6 kJ $mol^{-1}$, and the $E_a$ values calculated by KAS method were 129.3 and 210.7 kJ $mol^{-1}$. The differential and integral reaction mechanism functions of ignition reactions were determined, respectively, by $z(\alpha)$ master plots method, $f_1(\alpha)=2(1-\alpha)[-\ln(1-\alpha)]^{1/2}$, $g_1(\alpha)=[-\ln(1-\alpha)]^{1/2}$ ($B_4C/KNO_3$), and $f_2(\alpha)=3(1-\alpha)[-\ln(1-\alpha)]^{2/3}$, $g_2(\alpha)=[-\ln(1-\alpha)]^{1/3}$ ($B_4C/$

$KClO_4$). The pre-exponential factors, ln*A* values, were calculated using the intercepts of the fitting lines for KAS method. The ln*A* values of ignition reaction of $B_4C/KNO_3$ and $B_4C/KClO_4$ pyrotechnics were 11.6 and 22.4 $min^{-1}$. The results show that $B_4C/KNO_3$ has high thermal sensitivity and fast burning rate. This composition can be considered for making smoke composition products with adjustable burning rate and both visible and infrared obscuring. $B_4C/KClO_4$ with low thermal sensitivity and low burning rate can be mixed with suitable binder and used directly to make visible obscuring products.

**Acknowledgements** The support for this work was provided by the National Natural Science Foundation of China (Project No. 51676100).

## References

1. Eaton JC, Lopinto RJ, Palmer WG. Health effects of hexachloroethane (HC) smoke; accession number ADA277838; Defense Technical Information Center (DTIC): Fort Belvoir, VA, 1994; pp 1–60.
2. Shaw AP, Poret JC, Gilbert RA, et al. Development and performance of boron carbide-based smoke compositions. Propellants Explos Pyrotech. 2013;38(5):622–8.
3. Shaw AP, Diviacchi G, Black EL, et al. Versatile boron carbide-based visual obscurant compositions for smoke munitions. ACS Sustain Chem Eng. 2015;3(6):150423154904007.
4. Thévenot F. Boron carbide—a comprehensive review. J Eur Ceram Soc. 1990;6(4):205–25.
5. Reddy RG, Wang T, Mantha D. Thermodynamic properties of potassium nitrate–magnesium nitrate compound [$2KNO_3{\cdot}Mg(NO_3)_2$]. Thermochim Acta. 2012;531:6–11.
6. Benenson W, Harris JW, Stocker H et al. Handbook of physics; 2002. ISBN 978-0387952697.
7. Pan GP, Yang S. Pyrotechnic technology. Nanjing: Initiators and Pyrotechnics Technology Committee; 1995.
8. Wendlandt WW. Thermal analysis. 3rd ed. Hoboken: Wiley; 1986.
9. Vyazovkin S, Burnham AK, Criado JM, et al. ICTAC Kinetics Committee recommendations for performing kinetic computations on thermal analysis data. Thermochim Acta. 2011;520(1–2):1–19.
10. Pouretedal HR, Loh Mousavi S. Study of the ratio of fuel to oxidant on the kinetic of ignition reaction of Mg/$Ba(NO_3)_2$ and Mg/$Sr(NO_3)_2$ pyrotechnics by non-isothermal TG/DSC technique. J Therm Anal Calorim. 2018;132:1307–15.
11. Vyazovkin S. Alternative description of process kinetics. Thermochim Acta. 1992;211(1):181–7.
12. Flynn JH. The 'temperature integral'—its use and abuse. Thermochim Acta. 1997;300(1–2):83–92.
13. Miyata K. Combustion of boron-pyrotechnics. In: Joint propulsion conference and exhibit. 2013.
14. El-Awad AM. Catalytic effect of some chromites on the thermal decomposition of $KClO_4$ mechanistic and non-isothermal kinetic studies. J Therm Anal Calorim. 2000;61(1):197–208.
15. Liu PJ, Liu LL, He GQ. Effect of solid oxidizers on the thermal oxidation and combustion performance of amorphous boron. J Therm Anal Calorim. 2016;124(3):1587–93.
16. Ozawa T. A new method of analyzing thermogravimetric data. Bull Chem Soc Jpn. 1965;38:1881.
17. Flynn JH, Wall LA. General treatment of the thermogravimetry of polymers. J Res Natl Bureau Stand Part A. 1966;70:487.
18. Kissinger HE. Reaction kinetics in differential thermal analysis. Anal Chem. 1957;29(11):1702–6.
19. Akahira T, Sunose T. Method of determining activation deterioration constant of electrical insulating materials. Res Rep (Chiba Inst Technol) Sci Technol. 1971;16:22–31.
20. Malek J. The applicability of Johnson–Mehl–Avrami model in the thermal analysis of the crystallization kinetics of glasses. Thermochim Acta. 1995;267:61–73.
21. Brown ME. Introduction to thermal analysis. 2nd ed. Dodrecht: Kluwer; 2001.
22. Pouretedal HR, Ebadpour R. Application of Non-isothermal thermogravimetric method to interpret the decomposition kinetics of $NaNO_3$, $KNO_3$, and $KClO_4$. Int J Thermophys. 2014;35(5):942–51.